REPORT DOCUMENTATION PAGE

Form Approved
OMB No. 0704-0188

1. REPORT DATE *(DD-MM-YYYY)*	2. REPORT TYPE	3. DATES COVERED *(From - To)*
08/02/2019	Final Technical Report	06/01/2015 - 05/31/2018

4. TITLE AND SUBTITLE
All-Electronic Charge Storage Devices with Large Energy Density and Small Leak Currents

5a. CONTRACT NUMBER

5b. GRANT NUMBER
N00014-15-1-2397

5c. PROGRAM ELEMENT NUMBER
ONRFOA 14-012

6. AUTHOR(S)
Alfred Hubler and Alexey Bezryadin

5d. PROJECT NUMBER

5e. TASK NUMBER

5f. WORK UNIT NUMBER

7. PERFORMING ORGANIZATION NAME(S) AND ADDRESS(ES)
The Board of Trustees of the University of Illinois
Henry Administration Building
506 S. Wright St.
Urbana, Illinois 61801-3620

8. PERFORMING ORGANIZATION REPORT NUMBER

9. SPONSORING/MONITORING AGENCY NAME(S) AND ADDRESS(ES)
Office of Naval Research
875 N. Randolph St.
Arlington, VA 22217

10. SPONSOR/MONITOR'S ACRONYM(S)
ONR

11. SPONSOR/MONITOR'S REPORT NUMBER(S)

12. DISTRIBUTION/AVAILABILITY STATEMENT
Approved for Public Release; Distribution is Unlimited

13. SUPPLEMENTARY NOTES
The original PI for this award was Dr. Alfred Hubler. Dr. Hubler passed away on 1/27/18. Dr. Alexey Bezryadin assumed responsibility for the award and completed the research and report. ONRFOA 14-012 (FY15 Department of Defense MURI).

14. ABSTRACT
Electric capacitors are commonly used in electronic circuits for the short-term storage of small amounts of energy. It is desirable, however, to use capacitors to store much larger energy amounts to replace rechargeable batteries. Thus, we have developed, fabricated, and tested graphene nanocapacitors. The results indicate that such nanocapacitors can store an increased amount of energy because of the volume charge, can function in a wide temperature interval, have corresponding energy density that is 10 to 100 times larger than the energy density of a common electrolytic capacitor, and can store a charge in the dielectric layer equal to or in excess of the amount stored on the capacitor plates.

15. SUBJECT TERMS
capacitor, nanocapacitor, dielectric, electronic charge storage device

16. SECURITY CLASSIFICATION OF:			17. LIMITATION OF ABSTRACT	18. NUMBER OF PAGES	19a. NAME OF RESPONSIBLE PERSON
a. REPORT	b. ABSTRACT	c. THIS PAGE			Alexey Bezryadin (bezryadi@illinois.edu)
					19b. TELEPHONE NUMBER *(Include area code)*
U	U	U	UU	23	217-333-9580

FINAL REPORT

Grant: Office of Naval Research N00014-15-1-2397

PI: Alfred Hubler, University of Illinois at Urbana-Champaign

Co-PI: Alexey Bezryadin, University of Illinois at Urbana-Champaign

Title: All-electronic charge storage devices with large energy density and small leak currents

SUMMARY:

Electric capacitors are commonly used in electronic circuits for the short-term storage of small amounts of energy. It is desirable, however, to use capacitors to store much larger energy amounts to replace rechargeable batteries. Unfortunately, existing capacitors cannot store sufficient energy to be able to replace common electrochemical energy storage systems. Thus, we have developed, fabricated, and tested graphene nanocapacitors. The results indicate that such nanocapacitors can store an increased amount of energy because of the volume charge. The nanocapacitors are tri-layer systems, involving an Al film, an Al_2O_3 dielectric layer, and a single layer of carbon atoms, i.e., graphene. These are purely electronic capacitors, and therefore they can function in a wide temperature interval. The capacitors show a high dielectric breakdown electric field strength, of the order of 1000 kV/mm (i.e., 1 GV/m), which is much larger than the table value of the Al_2O_3 dielectric strength. The corresponding energy density is 10 to 100 times larger than the energy density of a common electrolytic capacitor. Moreover, we discovered that the amount of charge stored in the dielectric layer can be equal to, or can even exceed, the amount of charge stored on the capacitor plates. The dielectric discharge current follows a power-law time dependence. We suggest a model to explain this behavior.

INTRODUCTION

During the past five years, nanotechnology has begun to enhance the density of electrical energy storage. Electrochemical batteries, electrostatic capacitors, and hybrid devices such as electrical double-layer capacitors, which make use of both electrochemical and electrostatic storage principles, have recently been improved by incorporating nano-scale features.

Conventional electric capacitors are typically considered to be not very promising candidates for energy storage applications, because the charge stored on the metal plates is limited by the breakdown threshold in the electric field strength, thus limiting the energy density to, at most, hundreds of J/kg. The use of capacitors as energy storage systems has received a substantial revival of interest recently, because of the possibility of large increases in energy density for capacitors having gap spacing between the plates on a nanometer scale. [1,2] The improvement is expected because in vacuum capacitors, the field enhancement factor, β, characterizing the local enhancement of the average electric field arising from surface defects, decreases with the gap. [3,4] Hence, capacitors having an insulating layer that is only a few nanometers thick, called "nanocapacitors," might be able to withstand much higher electric fields before a breakdown damages the dielectric. The stored energy density of these systems should be able to be increased, especially if advanced, light-weight materials, such as graphene, are used to make the capacitor plates.[5] Graphene is a smooth material, so the field enhancement factor should be low. Graphene has been used previously for making capacitors and other nanoscale devices.[6,7,8,9,10]

Nanocapacitors based on graphene or similar metallic nanomaterials capping a very thin dielectric layer have been a subject of active study. A theoretical study of quantum size effects between graphene electrodes and h-BN dielectrics was reported for vertical stacking [11] as well as for in-plane geometry. [12] Such capacitors have also been studied experimentally.[13,14,15,16,17]

For practical applications, it is conventionally assumed that most of the electric charge in a standard metal/insulator capacitor is stored on the metal plates. However, in a fully charged capacitor, some extra charge is usually stored in the dielectric layer separating the plates. The dielectric volume charge is usually neglected, since it is typically small—of the order of 1 % of the total charge accumulated in the capacitor. Such charge penetration into the dielectric is driven by the strong electric field occurring in the dielectric spacer of a nanocapacitor. Charging of the dielectric layer has been studied previously,[18,19,20] but not on graphene-based nanocapacitors. Generally, there are several competing mechanisms by which the energy can be retained in the dielectric layer. Two of them— hindered dipole rotation and displacement of electrons and/or ions in the dielectric—do not involve any transfer of charge between the metal plates and the dielectric.[19,20] Additionally, charge penetration into the dielectric could always occur from the movement of hopping charges, i.e., the tunneling of electrons between the metal plates and some localized charge traps in the dielectric.[21,22,23,] Moreover, even if new charges do not enter, the charges located on the traps or defects inside the dielectric can tunnel from one defect to another and thus shift their positions significantly to cause additional charge accumulation on the plates of the capacitor.

MAIN RESULTS:

We discovered that the energy stored in the dielectric layer can be equal to and can even exceed the energy stored on the plates of the capacitor. This fact offers a new way to expand the energy storage capability of nanocapacitors. This phenomenon occurs when the dielectric layer is very thin, typically about 7 nm of Al_2O_3. Thus, electrons can penetrate into the dielectric by means of

quantum tunneling and therefore can efficiently populate it. Moreover, this type of energy storage device is shown to be stable against accidental shorts of the capacitor plates. The removal of the charge accumulated by the dielectric is a relatively slow process, which is controlled by its internal charge dynamics, generally described by relaxation theory. [24] We find that even if the plates are shorted out and the charge is completely removed from them, we can still recover a charge from the dielectric that is about equal to the charge present on the plates before the discharge occurred. Finally, capacitance measurements of our graphene nanocapacitors exhibit a five-fold increase of the capacitance of the device at low frequencies. This fact is an indication of the extremely large charge storage on the dielectric layer, which is characterized by comparatively slow charging and discharging.

1. We combined a nanoscale dielectric layer and a graphene capacitor plate in one device and achieved an enhanced energy density. Based on detailed measurements, we conjecture that a large amount of energy can be stored inside the dielectric. Namely, we estimate that the amount of charge and energy stored in the dielectric layer is about the same as the amount of charge and energy stored on the capacitor plates.
2. We present a simple and transparent model of the charge storage that offers a semi-quantitative explanation of the observed dependence of the discharge current, I_d, versus time, t. The release of the charge stored in the dielectric produces a discharge current that decreases with time as a power-law, $I_d \sim t^{-\alpha}$, where $\alpha \approx 1$, i.e., the current generated by the dielectric layer of the capacitor is inversely proportional to the time of discharge (approximately). On the other hand, the charge stored on the plates is released more quickly, generating an exponentially decreasing function of time, as expected.

NEWLY DEVELOPED FABIRACTION APPROACH:

The typical nanocapacitors used in this study were made with an 8-nm to 12-nm thick Al film coated by a 5-nm to 10-nm film of Al_2O_3 (the dielectric) and a single layer of graphene placed on top of the oxide. The oxide was deposited using a commercial atomic layer deposition (ALD) system (Savannah S100 Atomic layer deposition [Cambridge Nanotech]). Graphene layers were deposited using "*Trivial Transfer Graphene*" kits provided by *ACS Material*.

A schematic of the sample, image of the sample, and the measurement scheme are shown in Fig.1. The sample contains multiple Al electrodes (Fig.1b, c), any pair of which can be used as a unique double-capacitor (e.g., 1 and 2). The length of the graphene-covered section of each Al electrode is $L = 5$ nm or 10 mm, and the width of each Al strip is $w = 0.75$ mm.

As is clear from Fig.1, the device is not just a single capacitor of the type Al-Al_2O_3-G, but, rather, it is composed of two nominally identical capacitors connected in series through the graphene film in the middle. This is because, in the current realization, we do not make a contact to the graphene; both contacts are made to two Al strips, say #1 and #2. The capacitor on the left electrode (#1) of the device has a structure Al (green) - Al2O3 (red) – graphene (blue). The capacitor on the next electrode (#2) has the same structure, so the entire sequence is Al-Al_2O_3-G---G-Al_2O_3-Al. Such a design allows us to avoid making a direct contact to the graphene layer, which is quite fragile. The resulting devices are called "double-capacitors," since they represent two capacitors connected in series. The gap between the Al electrodes is 1-mm wide, and the resistance of the graphene in the middle, between the two capacitors, is of the order of 1 kΩ. Since the capacitance of the sample is of the order of C ~10 nF, the fastest discharge time is of the order of 10 μs if the leads are short-circuited.

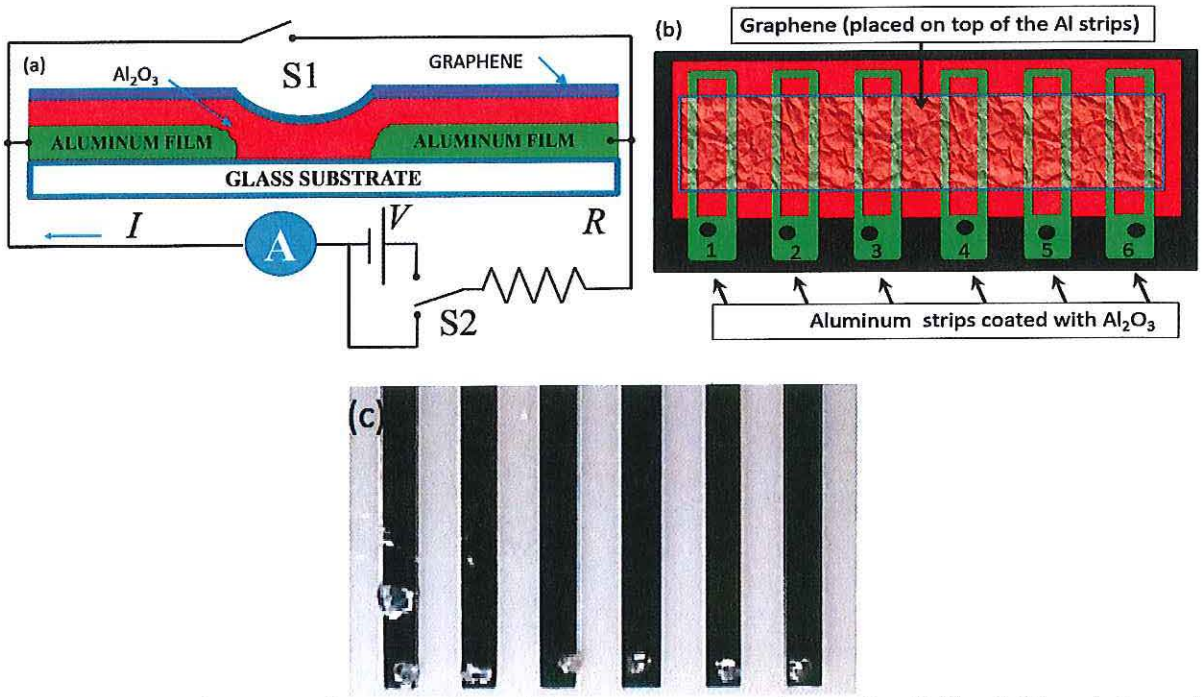

Figure 1. (a) Schematic of the sample and the measurement scheme. An Al film (~10 nm) (green) is deposited on a glass substrate (white) and covered with alumina (Al_2O_3) (~10 nm) (red), which serves as the dielectric layer of the capacitor. The top electrode is a single monolithic layer of graphene (blue). Graphene has metallic conductivity and acts here as the top metallic plate of the capacitors. The width of the Al electrodes is 0.75 mm, and the gap between them is 1 mm. Switch S1 is used to instantaneously discharge the capacitor plates. Switch S2 allows the capacitor to be charged through resistor R or discharged through the same resistor. (b) Top view of the nano-capacitors. Connections are made to the Al strips (but not to graphene), e.g., #1 and #2. Thus, effectively, the sample consists of two identical capacitors of the type Al-Al_2O_3-graphene, connected in series. Possible positions of the electrical contacts (indium dots) to the double-capacitor are shown by black circles. (c) Image of the sample. The black strips are the Al electrode, Indium dots, used to make contacts to the electrodes, are visible at the bottom. Graphene, which is placed in the central part of the sample, is too thin to be visible in this image.

TECHNICAL DESCRIPTION OF THE RESULTS OBTAINED:

Type I measurement: In the Type I measurement, we observed both the charge on the capacitor plates and the charge stored in the dielectric in the same measurement run. In this case, switch S1 was always open (i.e., disconnected). First, we charged the capacitor up to some voltage V, typically V=3V. The voltage was supplied by a Keithley 6517 electrometer; the same device was used to measure the current (marked "A" in the diagram). To charge the capacitor, switch S2 was connected upward (Fig.1a). After the capacitor was fully charged, switch S2 was connected downward (so that the voltage source was excluded from the circuit), and the discharge current was measured as a function of time (Fig.2; red curve). The discharging rates were limited by the resistor R. If R was sufficiently large (e.g., 100 MΩ or 1 GΩ), the discharge took many seconds and was easily measured using the Keithley 6517. Thus, the Type I measurement produced the results shown in Fig.2. This type of measurement, as discussed in detail later, shows that the discharging process occurs in two distinct stages. During the first stage, the capacitor plates

discharge exponentially. During the second stage, discharge from the charges stored in the dielectric film separates the capacitor plates. This second stage is a slower process, controlled by the insulator's internal charge dynamics. The discharge current obeys a power law, as illustrated by the linear dashed fitting line (Fig.2). Note that a power-law dependence appears linear in the log-log axis format.

Type II measurement: A second type of measurement algorithm was used to quantify, exclusively, the charge stored in the dielectric, Q_d. For this purpose, we first charged the capacitor fully. We then opened switch S1, connected switch S2 upward, and applied a voltage V for a time of ~10 min (Fig.1a). When charging was complete, switch S2 was turned downward, to exclude the charging voltage source. Then, immediately after, switch S1 was used to short-circuit the capacitor plates to remove all of the charge stored on them (i.e., Al strips and graphene film). Since switch S1 was on, the charge stored on the capacitor plates discharged nearly instantaneously (within ~10 μs). After the capacitor discharged, switch S1 was set again to "off"; i.e., the path to short-circuiting the plates was removed. At this point, switch S2 was still connected downward, enabling a discharge circuit involving the capacitor, the ammeter, and the resistor, all connected in series. Thus, the current flowing between the sample capacitor plates was measured with the ammeter. If the charge had been stored only on the plates, and not also in the dielectric, then the current would have been exactly zero, since the plates were fully discharged at time $t = 0$ when the measurement began. Yet, as we discuss below (Fig.6), the measured current and the corresponding integrated charge were both quite large. In fact, the charge stored on the dielectric was approximately equal to, or even sometimes higher than, the charge stored on the plates.

First, we performed Type I measurements. The capacitor was charged from a voltage source at V=3V. Then the capacitor was allowed to discharge through the resistor R and the current I was measured. Typical results are shown in Fig.2. Each charging process exhibited two distinct stages. First, we observed the initial exponential discharge, representing the charge on the plates of the capacitor. Second, we measured a power-law dependence of the current at a time scale longer than ~10 s, which represents the charge stored in the dielectric layer of the capacitor (Fig.2).

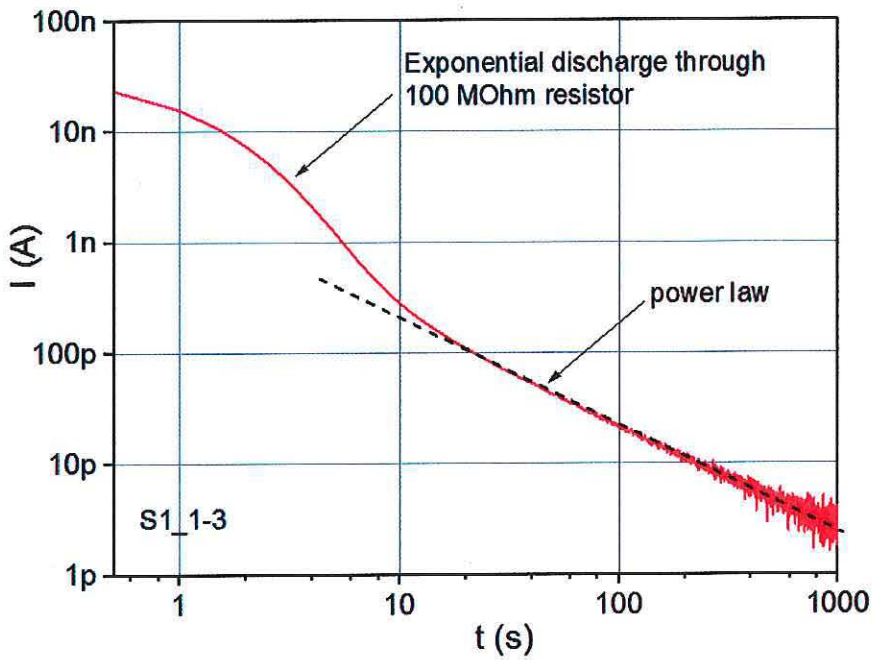

Figure 2. Sample S1_1-3. The discharge current is shown versus time, in log-log format. The capacitor was charged to 3 V before discharging. The discharge current flowed through a 100 MΩ resistor and an ammeter (Fig.1a). Initially, within the first 10 seconds or so, the discharge current dropped exponentially, as expected for an ideal capacitor shunted by a resistor. At longer time intervals, the current followed a power law I~1/t. This process is associated with the drainage of the charge stored in the dielectric layer of the capacitor.

The initial regime is exponential dependence, as expected for the discharge process of simple parallel-plate ideal capacitors. A numerical fitting shows that this dependence is well described by an exponent, initially, as confirmed by the fits in Fig.3 (dashed blue curve). There, the large black circles represent a discharge process through the resistor R. The time scale t-t_2 corresponds to the time elapsed from the beginning of the discharge process. The time interval t_2 is the delay between the end of the charging process and the beginning of discharging. During the time interval t_2, the sample was completely disconnected from any circuit (this was done to see how reliable the charge storage is on this type of capacitor). The fit is shown by the blue dashed line and corresponds to the expected exponential decrease of the current as $I(t)=V(t)/R=Q(t)/RC=[V(t_0)/R]*\exp[-(t-t_0)/\tau]$, where $\tau=RC$ is the time constant of the circuit including the resistor. Since the results represent a delayed measurement, the initial voltage is lower than the applied voltage, i.e., $V(t_0) < V(0) = 3$ V.

The fit (blue dashed line) agrees well with the data (black circles) up to the point where the current drops by a factor of about 20 when compared to its initial value, which corresponds to the discharge duration t-t_2~3s. This initial stage represents the discharging of the capacitor plates, the rate of which was limited by the resistor R. At longer time intervals, we observed current significantly exceeding the value expected from the exponentially decreasing fitting function. Moreover, at longer time intervals, i.e. t-t_2>3s, the current-versus-time dependence was approximately linear in the log-log plot. This fact suggests that at longer time intervals, a different energy storage mechanism is at play. This mechanism, as we discuss in detail below, represents

the charge stored inside the dielectric, and not on the plates of the capacitor. In subsequent sections, we will show that this charge is very significant and comparable to the charge stored on the capacitor plates.

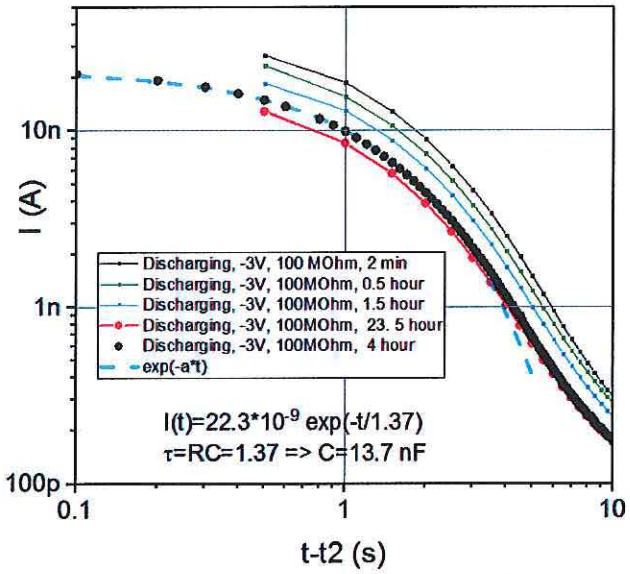

Figure 3. Sample S1_1-3. The discharge process of a double-nanocapacitor (see Fig.1), C, through a resistor R=100 MOhm. All of the curves represent delayed discharge measurements: After charging was completed, the capacitor was disconnected from all leads for a time interval t_2 to test the capacitor for internal leakage. At time t_2 the capacitor was connected to the ammeter through the resistor R and the discharge curve measured. The delay interval for the curves presented, from top to bottom, was t_2=2 min, 0.5 h, 1.5 h, 4 h, and 23.5 h. At $t=t_2$ the capacitor was connected to the ammeter through the resistor R and the current was measured versus time. The measurements are shown as symbols that are connected by lines, except the curve corresponding to t_2=4 h, a measurement that is shown instead by black circles. The exponential time-dependent fit (blue dashed curve) is shown for the case of t_2=4 h. The initial current was 22.3 nA, according to the fit, which corresponds to the initial voltage of 2.23 V (after a 4 h waiting period with disconnected leads).

The initial exponential fit allowed us to determine the capacitance of the sample. The fitting function and the fitting parameters are shown in Fig.3. The time constant is $\tau=RC$=1.37s. Since $R=10^8$ Ω, the capacitance is C=13.7 nF. Let us compare this value to the theoretical value, $C=(1/2)\varepsilon\varepsilon_0 Lw/d$, which is expected from the sample geometry. Here ε_0 is the permittivity of vacuum, and ε~9 is the dielectric constant of aluminum oxide. For the sample in Fig.3 (sample S1_1-3), the length of the electrodes was L~10 mm and the width was w~0.75 mm. The thickness of the dielectric (Al_2O_3) was d~10 nm. The factor 1/2 is included, because in our samples two nominally identical capacitors were connected in series. Thus we get C~30 nF. This estimate is somewhat larger than the measured value. We ascribe the difference to the expectation that the dielectric constant of the aluminum oxide was reduced at nanoscale, due to disorder, since our dielectric films were amorphous.

INTERNAL LEAKAGE:

For energy storage applications, the capacitor must hold its charge for extended periods of time. Energy loss is mainly caused by internal leakage between the plates of the capacitor, through the layer of the dielectric. The standard value for the resistivity of Al_2O_3 is 10^{14} Ω or larger. For our geometry (sample S1_1-3), the corresponding resistance of the capacitor dielectric layer was $R_C \sim 10^{11}$ Ω; the corresponding internal time constant would be $\tau_i = R_C C \sim 30$ min. We will see below that the actual measured internal discharge times are even better than this estimate.

Let us compare this estimate to the experimental values, which can be found from the data in Fig.3. The black circles represent a discharge current-versus-time curve measured after a delay of t_2=4 hours. In this experiment, the capacitor was charged to 3 V, then disconnected from the circuit completely. While disconnected, only internal leakage contributed to capacitor discharge. After 4 hours, the sample was reconnected to the measurement circuit (Fig.1), and the discharge curve was measured with a series resistor of 100 MΩ. The fit (Fig.3, blue dashed curve) gives us the value of the current at the beginning of the discharge curve measurement, which was $I(t_2)$=22.3 nA. Thus, the voltage on the capacitor plates, after the waiting period of 4 hours, was $V(t_2)=RI(t_2)$=22.3nA*100 MΩ=2.23V. Since the initial voltage was $V(0)$=3V, the internal leakage time τ_i is estimated as $\tau_i = t_2/\ln[V(0)/V(t_2)]$=13 h. This result was much better than the above estimate, suggesting that the effective resistivity of our nanometer-thick Al_2O_3 dielectric is about 10^{15} Ω (or somewhat higher), indicating the excellent quality of our ALD oxide.

Another, similar way to estimate the leakage of the charge through the dielectric is to compare the discharge curves measured after the t_2=4 h waiting period and the t_2=23.5 h waiting period (red circles), plotted in Fig.3. Each discharge curve is $V(t)=V_0(t_2)*\exp[-(t-t_2)/\tau]$, where $\tau=RC$ is the discharge time defined by the series resistor R. As discussed above, the internal leakage was described by its own exponent $V_0(t_2)=V_0(0)*\exp[-t_2/\tau_i]$, where t_2 is the duration when the capacitor was disconnected from the circuit completely. In other words, t_2 is the time interval between the moment when capacitor finished charging and the time when its discharge started due to its being connecting to the resistor and ammeter. Discharge through the dielectric layer will be called "internal discharge." Discharge through the resistor will be called "controlled discharge." The controlled discharge goes much faster than the internal discharge, since the resistor value is much lower than the dielectric layer's leakage resistance.

The controlled discharge current is $I_b(t-t_{2b})=[V_0(t_{2b})/R]*\exp[-(t-t_{2b})/\tau]$ for the black-circle curve and $I_r(t-t_{2r})=[V_0(t_{2r})/R]*\exp[-(t-t_{2r})/\tau]$ for the red-circle curve. Here t_{2b}=4 h and t_{2r}=23.5 h. To compare the black-circle and the red-circle measurements in Fig.3, we chose the same controlled discharge duration on both curves—namely $t-t_{2r}=t-t_{2b}$=0.5 s—since the current at this time was relatively high and the corresponding data point was available on both curves. The ratio of the controlled discharge currents is $I_b(t-t_{2b})/I_r(t-t_{2r})=[V_0(t_{2b})/V_0(t_{2r})]*\{\exp[-(t-t_{2r})/\tau]/\exp[-(t-t_{2b})/\tau\}=V_0(t_{2b})/V_0(t_{2r})$. We assumed that the voltage at the beginning of the controlled discharge would be reduced due to the preceding spontaneous discharge according to the usual discharge formula: $V_0(t_{2b})=V_0(0)*\exp[-t_{2b}/\tau_i]$ and $V_0(t_{2r})=V_0(0)*\exp[-t_{2r}/\tau_i]$. So $V_0(t_{2b})/V_0(t_{2r})=\exp[(t_{2r}-t_{2b})/\tau_i]$ and $I_b(t-t_{2b})/I_r(t-t_{2r})=\exp[(t_{2r}-t_{2b})/\tau_i]$. Finally, we get a relationship between the internal discharge time constant and the initial current in the controlled discharge measurement as follows: $\tau_i=(t_{2r}-t_{2b})/\ln(I_b(t-t_{2b})/I_r(t-t_{2r}))$. Thus, we get the internal discharge time constant τ_i=135h. The results suggest that the capacitor can be used to store a charge for many days. This time is longer than the independent estimate given above, because the discharge might go faster when the voltage is higher.

BULK CHARGE MEASUREMENTS:

The most significant result of this work is the observation of a large additional charge, Q_d, stored in the dielectric layer of the capacitor. We found that the charge Q_d accumulated by the layer of aluminum oxide is approximately equal to, and sometimes even larger than, the charge $Q_p=CV$, stored on the plates of the capacitor. Here, C is the geometric capacitance. These two charges, Q_p and Q_d, can be measured separately, since the discharge of the capacitor plates is an exponential function of time, with the time constant controlled by the resistor R shunting the capacitor. The discharge of the dielectric-stored charge Q_d is a much slower process, usually described by a power-law dependence on time. The dielectric charge release rate is limited by the charge migration dynamics inside the dielectric layer.

A. Exponential Fitting Analysis: Here we present an example of the data analysis intended to quantify the charge stored on the dielectric. To achieve this analysis, we first quantify Q_p. The charge on the capacitor metal plates, Q_p, is well defined, since it follows an exponential dependence on time if the capacitor is charged or discharged through a calibrated resistor. The current flowing to the capacitor plates can be fitted with an exponential function, which can be easily extrapolated to the entire time interval, from zero to infinity, and integrated analytically. The total charge is estimated using the numerical integration of the total current as the capacitor is charged. As we discuss below, the charging current follows the expected exponential function initially, but it exceeds the exponential function at long time intervals.

In this test we applied a bias voltage of 3V to a double-capacitor through a series resistor resister of R=1 GΩ and measured the current as a function of time, $I(t)$ (Fig.4). The schematic of the experiment in the test discussed here is shown in Fig.1, with switch S1 open. The initial charge on the capacitor was zero. At t=0 a voltage was applied, V=3V, which resulted in a charging current that decreased with time as the voltage on the capacitor increased. An example of such a measurement is shown in Fig.4. There, the data are shown as black squares; the blue straight line is the best exponential fit corresponding to the initial part of the plot, $I_{fit}=I_0\exp(-t/\tau)$. The fitting constants are I_0=2.911 nA and τ=10.06 s. The key observation here is that the charging current decreased more slowly than an exponential rate, except for the initial region, which had a duration of a few seconds. This fact indicates that, in addition to charging the plates of the capacitor, the dielectric was also being charged. Below, we explain how the charge stored on the dielectric can be evaluated numerically. The general approach is to first determine the charge on the plates of the capacitor, Q_p, by integrating the best-fit exponent. Then we integrate the entire $I(t)$ curve and find the total charge Q_t. Finally, the charge on the dielectric layer is naturally calculated as $Q_d=Q_t-Q_p$.

The charge on the plates is defined by a simple integral of the exponent, namely $Q_p=I_0\int\exp(-t/\tau)dt$. To find the complete charge that flows into the capacitor plates, the integral must be evaluated over the entire time axis, namely from zero to infinity (charging is assumed to begin at t=0). The result is $Q_p=I_0\tau$=29.3 nC. Another way to check this result is to find the corresponding capacitance as $C=\tau/R$=10.06 nF and to use this value to determine the charge of the capacitor, which is $Q_p=CV$=30.2 nC. The results are similar to those obtained above.

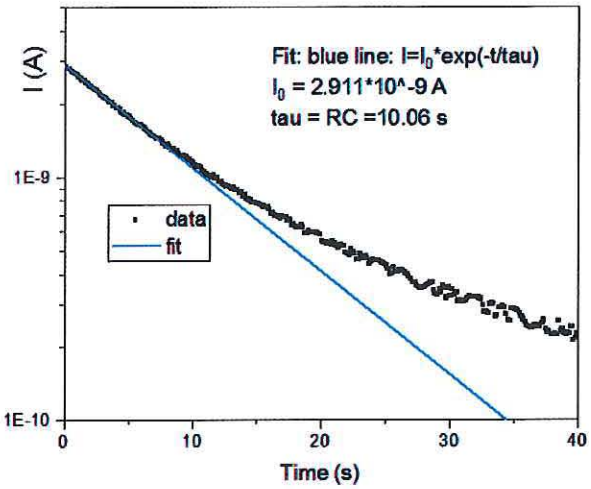

Figure 4. Sample S1_2-3. The charging current as a function of time for the graphene double-capacitor sample of Fig.1, with series resistor and voltage being R=1GΩ and V=3V. The blue line represents the best exponential fit. The measured current (black squares) appears higher than the expected exponential behavior (blue line), indicating that a significant portion of the current is flowing into the dielectric layer and charging it. The dielectric charge is estimated (see text) to be even higher than the charge localized on the plates of the capacitor.

The next step of the analysis is the integration of the measured charging curve, $I(t)$. A straightforward numerical integration gives the total charge $Q_{t,raw}$=132 nC. We label this estimated charge as "raw" or "uncorrected" for two reasons. First, the device used to measure current might have an offset of zero. In fact, some offset current is present in any measurement apparatus due to the finite accuracy of any device. A small offset is normally not a big problem, but since the charge in the present case is evaluated by means of integration, the total charge might appear exaggerated. Second, when voltage is applied, some leakage current might flow through the insulating layer. Again, if the integration is sufficiently long, both the offset and the leakage currents can lead to an overestimated total charge. To compensate for these two effects, we performed a lower bound estimate of the total charge stored. For this purpose, we estimate the total charge as $Q_t=\int[I(t)-I_{offset}]dt$. Here the offset current is evaluated as a mean value current at times near the end of the integration interval. In the example of Fig.4, such a corrected charge is Q_t=74.6 nC, while the estimated current offset is I_0=13 pA. Taking into account the above estimate of the charge on the plates, we can now find the charge stored in the dielectric film of the capacitor as $Q_d=Q_t-Q_p$= 41.3. Finally, we introduce the efficiency of the dielectric layer to store charge, defined as $Eff=Q_d/Q_p$=1.4.

For comparison we measured a commercially available ceramic capacitor (10 nF, 1kV, Z5U) using the same setup. The observed efficiency of the dielectric storage was determined to occur between Eff=0.02 and Eff=0.025 (for the bias voltage varying in the range 5-20 V), which is much lower than the value observed on our graphene nanocapacitors.

B. Integration Analysis: In this example, the sample was charged up to 3V, and then the discharge current was measured through a resistor of 100 MΩ.

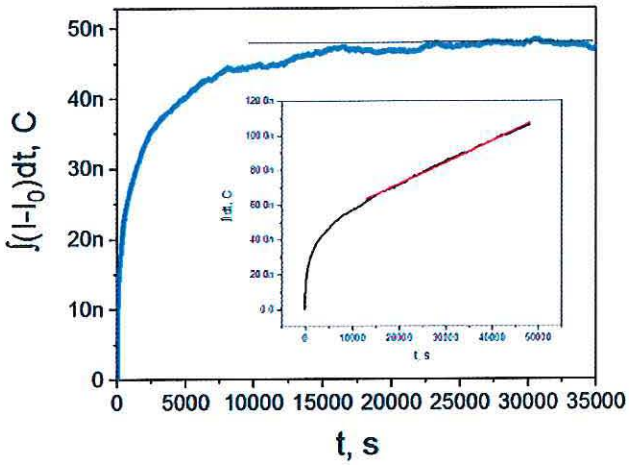

Fig.5. Insert: The total charge of the capacitor obtained by the numerical integration of a corresponding current-versus-time curve measured in the discharge process. The linear segment at long time intervals is due to the offset current. Main figure: Integral of the total current, from which the offset current is subtracted. In this case, the total charge converges to a constant value at a long time interval, which is about 47 nC. This is a lower-bound estimate of the charge stored on the capacitor.

The current-versus-time dependence was integrated to produce the charge-versus-time plot of Fig.5 (insert). Here, the most pronounced feature is the linear increase of the net charge with time, at times larger than ~15000 c. Given that the capacitor's accumulation of a charge does not have a physical cause, this linear increase must be corrected. The explanation is again the offset current. The offset current can be determined as the slope of the linear segment observed at long time intervals (Fig.5, insert). If the offset current is subtracted from the total current, then the integral converges to a constant. This limiting charge is a lower-bound estimate of the total charge stored. The result is given in Fig.5. The total charge is estimated at Q_t=47 nC. The time constant measured in this experiment was 1.3 s. The resistor was R=100 MΩ. Thus, the electric capacitance between the plates is 13 nF. The initial voltage was 2.26 V, and, correspondingly, the charge on the plates was Q_p=29.4nC. Therefore the efficiency in this measurement was found to be Eff=0.6, which is still much larger than has been observed in common ceramic capacitors, for example.

C. Type II measurements, power law dependence, and the dielectric charge storage estimate: In the experiments above, some charge was present on the plates and some charge was present in the dielectric. Thus, the disentanglement of these charges had to be carefully addressed. To simplify the analysis and to further confirm our conclusions, we present here a complementary test in which the charge on the capacitor plates was eliminated completely before measurement began. The steps of the measurement were as follows: (1) The capacitor was initially charged to a voltage V (1V, or 3V, or 5V) by switching S2 to the downward position. (2) Switch S2 was then changed upward. (3) The plates of the capacitor were shorted by closing switch S1 (Fig.1) for approximately one second. Note that the estimated discharge time, with switch S1 closed, was ~10 microseconds (see above). (4) Next, switch S1 was opened, so it no longer played a role. (5) Given that S2 was switched upward in Step #2, the capacitor was already connected to the ammeter through a series resistor R (Fig.1). The discharge current was measured. Under these conditions, this measurement represents the current, I_d, flowing from the dielectric. Since the plates had been discharged completely before the measurement, I_p=0 and Q_p=0. The results are shown in Fig.6,

with the plots presented in log-log format. Here the dots represent the measured points and the dashed lines are linear fits. The linear fit in the log-log format represents a power-law dependence. The curves measured after the capacitor was charged to 3V and 5V appear to agree with high accuracy with the dependence $I_d \sim 1/t$ (see red and blue data points). The dependence corresponding to the initial charging voltage of 1V appears to follow a power law $I_d \sim t^{-\alpha}$ with $\alpha \approx 1$, but, strictly speaking, $\alpha < 1$ in this case (α is in fact just slightly less than unity).

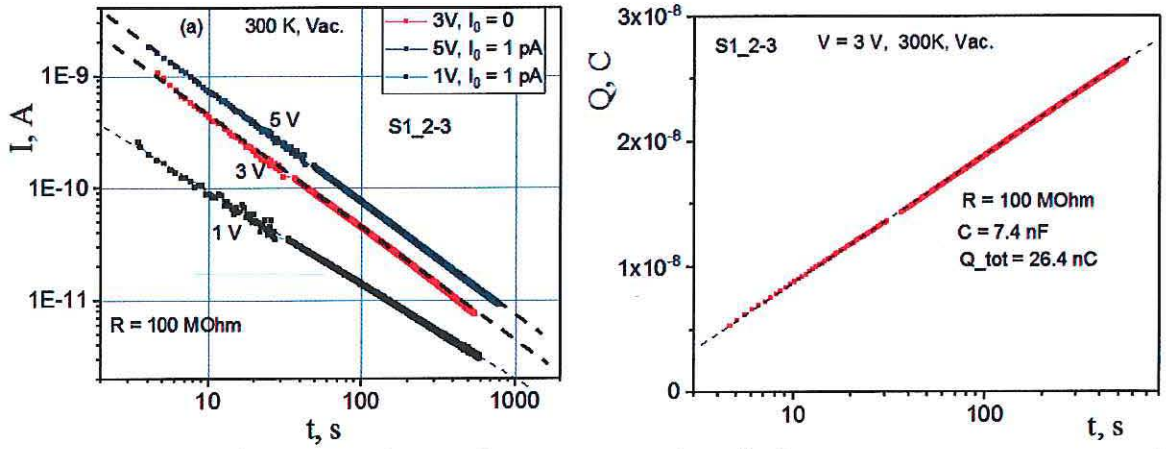

Figure 6. (a) Sample S1_2-3. The graphene nanocapacitor discharge process, current versus time, shown for three different voltages. The sample was measured in a vacuum. Before each measurement, the capacitor was charged and then the plates were shorted for one or two seconds to discharge them. The current occurs as an after-effect, which indicates that the removal of the charge on the plates (by connecting them for a short time) does not cause the nanocapacitor to lose all stored energy. In all three cases the discharge current-versus-time dependence is similar to I(t)~1/t. The exact power of this power law decay can be either slightly smaller or slightly larger than the generic value of -1. For example, the thin dashed line (V=1 V) represents a dependence $t^{-\alpha}$ where α is slightly smaller than 1. The results corresponding to V=3 V and V=5 V show an exact inverse proportionality I(t)=const/t. (b) Integral charge of the discharge curve measure at 3 V.

One would expect that an unusually large amount of charge could be stored on the dielectric layer, since the current follows a power-law dependence and the integral of a power-law dependence is divergent, either at zero or at infinity or both. To demonstrate this conclusion quantitatively, we integrated the current versus time. The result (Fig.6b) is a logarithmic dependence on time. We did not expect any significant contribution of the offset or leakage currents here—since the dependence at long time intervals is not linear—and this is what we found. The observed logarithmic dependence (which appears linear in the Fig.6b, since the x-axis is logarithmic) is exactly as expected when the current is $I \sim 1/t$, as the charge is the integral of the current over time.

To estimate the efficiency, we used the capacitance measured by a multimeter (LRC meter operating at 1kHz), which turned out to be 7.4 nF. The charging voltage was 3V (Fig.6b). Thus, the charge on the plates was $Q_p = CV = 22.2$ nC. The integrated charge in Fig.6b was $Q_d = 26.4$ nC, and the efficiency was therefore $Eff = Q_d/Q_p = 1.19$. Thus, in this example analysis, the charge stored on the dielectric appears higher than the charge stored on the plates of the capacitor.

Another conclusion that follows from the results of Fig.6 is that the system was stable against an accidental shorting of the plates of the capacitor. In Fig.6, the plates were shorted before the measurement. Yet, subsequent measurements demonstrate that the energy that remained on the capacitor, stored on the dielectric, was comparable to $CV^2/2$.

DISCUSSION:

Qualitatively speaking, the accumulation of the charge on the dielectric layer, reported here, resembles the phenomenon of creep.[25,26] In these examples, the creep phenomenon describes displacements of molecules. In the case considered here, electrons and/or ions (i.e., charged particles) might be experiencing creep. Thus, the current obeys a power law, in a general sense analogous to the findings in Ref. [27 and 28]. The logarithmic dependence has been also predicted, for a highly resistive granular system of partially oxidize Al film in Ref. [27].

Fundamentally, the time-dependent response of a system to a step-function removal of constant stress is most conveniently defined through the Fourier transform of the frequency-dependent response, which is known for a large variety of mechanisms of dielectric absorption. As suggested by Jonscher,[24] one can generally distinguish between two fundamentally different types of dielectric response.[27] The first type, termed "dipolar," is a generalization of the Debye concept of polarization due to the hindered movement of ideal dipoles. This type of polarization leads to zero residual polarization after discharge, with the time dependence of the charge described by the exponential law $\sim exp(-\omega_p t)$, where ω_p is the loss peak frequency of the dielectric response in the frequency domain. The second type of response describes the behavior of a system where polarization is dominated by slow movement of hopping charge carriers, which is relevant for the charge accumulation due to the tunneling of electrons to localized states in the dielectric. This type of dielectric response has a fractional power-law time dependence, $\sim t^{-\alpha}$, and is characterized by the finite residual polarization of the system.

In practical applications, the measured property is usually not the residual polarization or the residual charge but the discharge current. Generally, for times much longer than the RC relaxation time of the capacitor, the discharge current resulting from different charge-retention mechanisms in the dielectric can be described by the fractional power law $\sim t^{-\alpha}$, with different mechanisms generating different values of the power α.[6] The varying time dependence of the discharge currents resulting from different mechanisms of charge absorption can in principle be used to eliminate some mechanisms for a particular dielectric, or to analyze the relative contributions of those mechanisms. In addition to differing in time dependencies, some mechanisms differ in charging and discharging processes, which can be further used for the same purpose. Specifically, the trapped volume charge formed through charge injection, possibly by tunneling,[28] can be absorbed and released on different time scales, making its contribution apparent if a large hysteresis is observed between the charge and discharge currents.

Next, we estimate the energy density using the example of the sample S1_1-3, the parameters of which are given below Fig.3. The total energy is $E=CV^2/2\sim60$ nJ. If one takes into account the energy stored in the dielectric, then $E\sim100$ nJ. The energy density is $E/(Lwd)\sim1.3$ MJ/m^3. This result can be converted to energy per unit mass. The density of Al_2O_3 is 4 g/cm^3=4000kg/m^3. Thus, the mass of the dielectric layer is 0.3 nano-gramm, resulting in an energy density (per unit weight) of ~330 J/kg. This level of energy density is about an order of magnitude better than that of ordinary electrostatic capacitors. Here we adopt an optimistic point of view, assuming that both of the capacitor electrodes were made of graphene, the weight of which is negligible compared to the weight of the dielectric film. Such nanocapacitors can be used for

local energy storage—at cryogenic temperatures, for example, where ionic and electrolytic capacitors might not work.

CAPACITANCE VERSUS FREQUENCY:

The results presented above suggest that the charge stored in the dielectric is large, but it takes longer to extract it, compared to the capacitor plates. Thus, if the capacitance is measured at a sufficiently low frequency, its capacitance should be significantly larger than the capacitance measured at a higher frequency. We have tested this hypothesis using a commercial capacitance measurement setup, with an LCR HP4776 (100Hz – 20 kHz) and lock-in amplifier SR 830 for frequencies below 100Hz. The results are shown in Fig.7 for two similar samples.

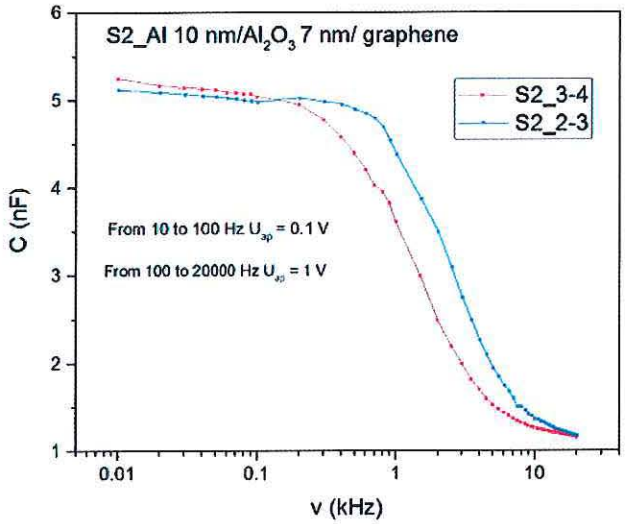

Figure 7. (a) Capacitance of a double-nanocapacitor with a graphene top electrode, measured versus frequency. A roughly five-fold increase of the capacitance was apparent as the frequency was reduced from ~10 kHz to ~10 Hz. The sample design is given in Fig.1.

The results show that the capacitance remained roughly constant in the interval 10-20 kHz. As the probe frequency was reduced from 10 kHz to 10 Hz, the effective capacitance of the sample increased by a factor five or so. The rapid growth stopped near 1 kHz. At lower frequencies, the capacitance continued to grow, but significantly more slowly, and, apparently, linearly, in the log-linear format of Fig.7. This linear increase, at frequencies lower than about 200 Hz, represents a logarithmic growth because the x-axis scale is logarithmic. The reported large storage capacity of the dielectric is related to the logarithmic increase of the capacitance at low frequencies (<200 Hz). Indeed, if $Q \sim \ln(t) \sim \ln(1/f)$, then $C=Q/V=C_0+C_1\ln(1/f)=C_0-C_1\ln(f)$, exactly as observed.

MODEL:

Quantum tunneling has been discussed previously as a mechanism that allows charge penetration into the dielectric layer.[29] Here we propose a simpler and more intuitive model, based on quantum tunneling, which assumes many impurities (rather than just one, as discussed in the above reference). As we will see, our model reproduces the power-law dependence observed in the discharge current, $I(t) \sim t^{-\alpha}$, with $\alpha \sim 1$.

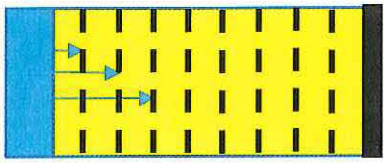

Figure 8. Proposed model. The capacitor is formed between a metallic Al film (blue) and a layer of graphene (black). The dielectric spacer between the plates (yellow) is Al_2O_3. The dashed lines show hypothetical charge traps. They are positioned along straight lines for the sake of an easier analysis. In reality, the position of the charge traps is random. We estimate that the number of traps is of the order of 1% of the total number of atoms in the dielectric layer. The distance between the dashed lines is d_p.

The model is illustrated in Fig.8. A plane capacitor was formed between two metallic plates (blue and black) and a dielectric spacer (yellow). The position of the charge traps is shown by dashed lines, schematically. For simplicity, we assumed that the charge traps were positioned along the dashed lines, their distance from the left metallic plate being $x_n=d_p*n$, where $n=1,2,3\ldots$ is an integer and d_p is the distance between trap planes. Let us assume that the left metallic plate is negatively biased and the electrons propagate to the right, into the dielectric, by means of quantum tunneling[16] (see the horizontal blue arrows). Note that the match between the energy of the incoming electron and the energy of the state localized in a trap does not have to be perfect since electrons exchange some energy with the thermal bath. All reported experiments were done at room temperature, to enable thermal fluctuations to help with tunneling between states with slightly different energies. Tunneling events can happen from the metallic plate to a trap inside the dielectric; they can also happen inside the dielectric, from one trap to a neighbor trap, but this possibility is not analyzed here. The probability of a tunneling event was controlled only by the distance over which the tunneling occurred, and not by the initial position of the electron.

According to the elementary theory of quantum tunneling, the tunneling probability to the first trap plane (top arrow, Fig.8) can be estimated as $p_1=C*\exp[-x_1/\xi]=C*\exp[-d_p/\xi]$. Here ξ is the localization length of the electronic wave function. The tunneling rate to the second layer (middle arrow, Fig.8) of charge traps was $p_2=C*\exp[-x_2/\xi]=C*\exp[-2d_p/\xi]$, because the second layer was removed from the initial location of the tunneling electrons by distance $2d_p$. The third layer was removed by a distance $3d_p$, so the corresponding tunneling rate (bottom arrow, Fig.8) was $p_3=C*\exp[-x_3/\xi]=C*\exp[-3d_p/\xi]$, etc. The rate of tunneling events occurring over a distance of n steps was $p_n=C*\exp[-x_n/\xi]=C*\exp[-nd_p/\xi]$. The underlying assumption here is that the relevant electronic states were localized, since they took place inside the dielectric layer.

Let us now assume that a voltage is applied and the electrons begin to tunnel into the dielectric or inside the dielectric, because the energy of the available traps is reduced and becomes comparable to the Fermi energy in the metallic electrode. Assume that we wait a time duration t and then estimate how many charge-trap planes are charged (filled with electrons). It can be said that the time interval needed to achieve a tunneling of an electron by n steps is $T_n\approx 1/p_n$. So within time t all possible electron tunneling events that are characterized by the condition $1/p_n<t$ will occur. The farthest charged penetration distance, $n_{max}(t)$, which will be filled within time t, is defined by the condition $T_n\approx t$, or $p_{n\_max}\approx 1/t$, or $C*\exp[-d_p n_{max}/\xi]\approx 1/t$. This can be solved to obtain $n_{max}=(\xi/d_p)\ln(tC)$. So the charge that can enter the dielectric within time t is $Q(t)=M_p*n_{max}$, where M_p is the number of traps per one trap plane. If the chosen number of planes on which the charges can shift is N_p, then $M_p=N_{trap}/N_p$, where N_{trap} is the total number of charge traps in the sample. The

number of layers has been chosen for simplicity, so N_p can be any integer number much larger than one. But N_p should not be too large, so that M_p is still much larger than unity. In this model the distance between the planes is $d_p=d/N_p$, where d is the total thickness of the dielectric.

We can now make a prediction for the total charge that enters the dielectric within time t, namely $Q(t)=M_p*n_{max}=(\xi M_p/d_p)\ln(tC)$ (n.b., this model is only applicable if t is sufficiently large so that the number of charged trap planes is larger than unity). Thus, the charging current should depend on time as follows: $I(t)=(dQ/dt)=(\xi M_p/d_p)(1/t)$. This is very similar to the experimental observations.

The same current, presumably, exits the dielectric since tunneling is reversible if the voltage is removed. Thus the discharge current should also be defined as $I(t)=(\xi M_p/d_p)(1/t)$. Our experimental tests confirm that the charging and discharging of current curves are very similar (not shown). The power dependence of the experimental discharge curves is indeed similar to the predicted $1/t$ dependence (Fig.6).

REFERENCES:

[1] D. Lyon & A. Hubler. Gap size dependence of the dielectric strength in nano vacuum gaps. *IEEE Trans. Dielectr. Electr. Insul.* **20**, 1467–1471 (2013).

[2] A. Hubler & O. Osuagwu. O. Digital quantum batteries: energy and information storage in nanovacuum tube arrays. *Complexity* **15**, 48–55 (2010).

[3] W. S. Boyle, P. Kisliuk, & L. H. Germer. Electrical breakdown in high vacuum. *J. Appl. Phys.* **26**, 720–725 (1955).

[4] D. Alpert, D. A. Lee, E. M. Lyman, & H. E. Tomaschke, Initiation of electrical breakdown in ultrahigh vacuum. *J. Vac. Sci. Technol.* **1**, 35-50 (1964).

[5] Y. Huang, J. Liang, & Y. Chen. An overview of the applications of graphene-based materials in supercapacitors. *Small* **8**, 1805 (2012).

[6] B. Balamuralitharan, S. N. Karthick, S. K. Balasingam, K. V. Hemalatha, S. Selvam, J. A. Raj, K. Prabakar, Y. Jun, & H. J. Kim. Hybrid reduced graphene oxide/manganese diselenide cubes: A new electrode material for supercapacitors. *J. Energy Technology* **5** (2017).

[7] Suresh Kannan Balasingam & Yongseok Jun. Recent progress on reduced graphene oxide-based counter electrodes for cost-effective dye-sensitized solar cells. *Israel Journal of Chemistry* **55**, 955–965 (2015).

[8] S. K. Balasingam, J. S. Lee, & Y. Jun. Molybdenum diselenide/reduced graphene oxide based hybrid nanosheets for supercapacitor applications. *Dalton Transactions* **45**, 9646–9653 (2016).

[9] M. Lee, S. K. Balasingam, Y. Ko, H. Y. Jeong, B. K. Min, Y. J. Yun, & Y. Jun. Graphene modified vanadium pentoxide nanobelts as an efficient counter electrode for dye-sensitized solar cells. *Synthetic Metals* **215**, 110–115 (2016).

[10] M. Lee, W. G. Hong, H. Y. Jeong, S. K. Balasingam, Z. Lee, S. J. Chang, B. H. Kim, & Y. Jun. Graphene oxide assisted spontaneous growth of V2O5nanowires at room temperature. *Nanoscale* **6**, 19, 11066–11071 (2014).

[11] V. O. Ozcelik & S. Ciraci. Nanoscale dielectric capacitors composed of graphene and boron nitride layers: A first-principles study of high capacitance at nanoscale. *J. Phys. Chem C* **117**, 15327 (2013).

[12] V. O. Ozcelik & S. Ciraci. High-performance planar nanoscale dielectric capacitors. *Phys. Rev. B* **91**, 195445 (2015).

[13] G. Shi, Y. Hanlumyuang, Z. Liu, Y. Gong, W. Gao, B. Li, J. Kono, J. Lou, R. Vajtai, P. Sharma, & P. M. Ajayan. Boron nitride-graphene nanocapacitor and the origins of anomalous size-dependent increase of capacitance. *Nano Letter* **14**, 1739 (2014).

[14] B. Bhattacharya & U. Sarkar. Graphyne-graphene (nitride) heterostructure as nanocapacitor. *Chemical Physics* **478**, 73 (2016).

[15] S. Byun, J. H. Kim, S. H. Song, M. Lee, J.-J. Park, G. Lee, S. H. Hong, & D. Lee. Ordered, scalable heterostructure comprising boron nitride and graphene for high-performance flexible supercapacitors. *Chem. Mater.* **28**, 7750 (2016).

[16] B. Bhattacharya, U. Sarkar, & N. Seriani. Electronic properties of homo- and heterobilayer graphyne: The idea of a nanocapacitor. *J. Phys. Chem. C* **120**, 26579 (2016).

[17] C. Zhang, Y. Zhang, P. Cummings, & D. Jiang. Computational insight into the capacitive performance of graphene edge planes. *Carbon* **116**, 278 (2017).

[18] H. J. Wintle. Absorption current, dielectric constant, and dielectric loss by the tunneling mechanism. *J. App. Phys.* **44**, 2514 (1973).

[19] B. Gross. On permanent charges in solid dielectrics. *J. Chem. Phys.* **11** 866 (1949).

[20] H. Gupta, K. Singh, T. John. Analysis of dielectric absorption in capacitors. *JAIR* **3** 255 (2014).

[21] D. K Das-Gupta. Conduction mechanisms and high-field effects in synthetic insulating polymers. *IEEE Trans. Dielectr. Electr. Insul.* **4**, 149 (1997).

[22] J. Lowell. Tunnelling between metals and insulators and its role in contact electrification *J. Phys. D* **12**, 1541 (1979).

[23] C. G. Garton. Charge transfer from metal to dielectric by contact potential. *J. Phys. D* **7**, 1814 (1974).

[24] A. K. Jonscher. Dielectric relaxation in solids. *J. Phys. D* **32,** R57 (1999).

[25] A. Zandiatashbar, C. R. Picu, & N. Koratkar. Control of epoxy creep using graphene. *Small* **8**, 1676–1682 (2012).

[26] D. Lee, S. H. Song, J. Hwang, S. H. Jin, K. H. Park, B. H. Kim, S. H. Hong, & S. Jeon. Enhanced mechanical properties of epoxy nanocomposites by mixing noncovalently functionalized boron nitride nano flakes. *Small* **9,** 2602–2610 (2013).

[27] G. Dreyfus & J. Lewiner. Electric fields and currents due to excess charges and dipoles in insulators. *Phys. Rev. B* **8**, 3032 (1973).

[28] B. Ricco, M. Ya Azbel, & M. H. Brodsky, Novel mechanism for tunneling and breakdown of thin Si02 films. *Phys. Rev. Lett.* **51**, 1795 (1983).

[29] H. J. Wintle. Absorption current, dielectric constant, and dielectric loss by the tunnelling mechanism. *J. Appl. Phys.* **44**, 2514 (1973).